

AN IMPROVED GUIDANCE ALGORITHM FOR SOLID PROPELLANT
BALLISTIC MISSILES

S.GHONIEMY * M.TANTAWY ** M.ELLEITHY ***

ABSTRACT

Due to production tolerances and off-nominal environmental conditions, the thrust time profile of solid propellant rocket motors suffers from high uncertainties in both magnitude and burn-out time. This behaviour leads to higher uncertainties in the motion parameters of the missile at the shut-off (burn-out) point. Accordingly, the impact point is highly erroneous. This paper develops a guidance and control strategy for compensating the effects of the above-mentioned uncertainties in such a way as to minimize impact errors.

-
- * Asc.Prof. Guid.Dep.M.T.C.
 - ** Asc.Prof. D.S.S.C.
 - *** Ph.D. Air Def.College

1-INTRODUCTION

The performance of ballistic missile systems is measured in three axes; namely: impact accuracy, maximum range, and destruction capability.

Impact accuracy is influenced mainly by:

- .Inertial measurement errors
- .Computation errors
- .Steering and burn out errors
- .Gravitational anomalies
- .Re-entry errors

Guidance and control strategies are designed to steer the missile on a reference trajectory (corresponding to a specified mission) for a specified state vector at shut-off to achieve suitable impact by minimization of the deviation of the missile from the target point.

Ballistic missile system designers have concentrated on the use of liquid propellant engines recognizing that their advantage is that they can be readily controlled. However, inherent advantage of handling ease has generated increased attention to the use of solid propellents. Due to production tolerances and off-nominal environmental conditions, the thrust time profile of solid propellant rocket motors suffers from high uncertainties in both magnitude and burn-out time. These uncertainties lead to higher uncertainties in the motion parameters of the missile at the shut-off (burn-out) point. Accordingly, the impact point is highly erroneous. This paper develops a guidance and control strategy for compensating the effects of the above mentioned uncertainties in such a way as to minimize impact errors.

2-MODELING AND SIMULATION

2.1-Reference Coordinates and Vector Transformations

The reference coordinate systems used through out this study are shown in Figure.1.

The transformation of a vector A in body coordinate system to a vector A_e in earth coordinate system is carried out through the matrix [ME]

$$[ME] = \begin{bmatrix} I_1 & J_1 & K_1 \\ I_2 & J_2 & K_2 \\ I_3 & J_3 & K_3 \end{bmatrix} ; [ME]^{-1} = [ME]^T = [EM]$$

This transformation contains three intermediate transformations;
- Missile-Fire
- Fire-Local , and
- Local-Earth
transformations.

2.2- Six degrees of Freedom Motion Equations

The vectorial system of equations describing the ballistic missile motion in space is as follows:

$$\begin{aligned} \dot{\bar{R}}_m &= \dot{\bar{R}}_m + \dot{\bar{W}}_e \wedge \bar{R}_m \\ \dot{\bar{V}}_e &= \dot{\bar{V}}_e + \dot{\bar{W}}_e \wedge \bar{V}_e = \bar{A}_e + \bar{G}_e \\ \dot{\bar{I}}_m &= (\dot{\bar{W}}_{me} - \dot{\bar{W}}_e) \wedge \bar{I}_m \\ \dot{\bar{J}}_m &= (\dot{\bar{W}}_{me} - \dot{\bar{W}}_e) \wedge \bar{J}_m \\ \dot{\bar{H}}_a + \dot{\bar{W}}_m \wedge \bar{H}_a &= \bar{T}_A + \bar{T}_T \\ \bar{A} &= (\bar{F}_A + \bar{F}_T) / m a s \\ \bar{K}_m &= \bar{I}_m \wedge \bar{J}_m \end{aligned}$$

2.3-Fire Plane Motion Equations

The fire plane is defined by the launch point, target point, and earth center. Under the assumptions that:

- the launch point is at (0,0)
- the target point is in the north direction
- the missile is roll stabilized such that $W_{x1}=0$
- the missile is of X-form
- the missile moves in the fire plane with $\Psi = \Psi_0 = 0 ; W_{y1}=0$

the equations of motion take the form:

$$\begin{aligned} \dot{x}_e &= v_{e1} & \dot{y}_e &= v_{e2} \\ \dot{v}_{e1} &= A_1 I_1 + A_2 J_1 + G_{e1} & \dot{v}_{e2} &= A_1 I_2 + A_2 J_2 + G_{e2} \\ \dot{I}_1 &= -W_{z1} I_2 (I_1 J_2 - I_2 J_1) & \dot{I}_2 &= W_{z1} I_1 (I_1 J_2 - I_2 J_1) \\ \dot{J}_1 &= -W_{z1} J_2 (I_1 J_2 - I_2 J_1) & \dot{J}_2 &= W_{z1} J_1 (I_1 J_2 - I_2 J_1) \\ \dot{W}_{z1} &= (T_{A3} + T_{T3}) / J_{22} \end{aligned}$$

With initial conditions:

$$\begin{aligned} x_e(0) &= 0 & y_e(0) &= R_e \\ v_{e1}(0) &= 0 & v_{e2}(0) &= 0 \\ I_1(0) &= \cos \theta_0 & I_2(0) &= \sin \theta_0 \\ J_1(0) &= -\sin \theta_0 & J_2(0) &= \cos \theta_0 \\ W_{z1}(0) &= 0 \end{aligned}$$

14-16 May 1991, CAIRO

2.4- Autopilot

To achieve adequate stability and reasonable rapid and well damped response with moderate insensitivity to external disturbances a lateral autopilot; Fig.2.; is designed to control the short period dynamics such that:

$$\dot{\delta}_z = -K_1 W_{z1} + K_2 V_{a2}/V_{a1} + K_3 \delta_z + U_d$$

where K_1, K_2, K_3 are determined through pole assignement technique.

2.5-Mission (Reference Trajectory)

The assumed mission is described through:

$$\Gamma_r = \text{constant} = \theta_0$$

$$\text{hence } \dot{\Gamma}_r = 0$$

2.6-Attitude Control

The attitude control demand is calculated by augmenting the difference between Γ_r and Γ through P.I. compensator. Fig-2 shows the functional block diagram for the closed loop ballistic missile system illustrating the additive compensators employed for improving both short and long period dynamics behaviour.

This system is simulated under the assumptions:

- . launch point is (0,0)
- . target point is in the north direction
- . $\theta_0 = (15, 30, 45, 60, \dots)$

and the results are shown in Figures 3 and 4.

-Fig.3 shows the actual mission for $\theta_0 = 60^\circ$ and for different rocket motors.

-Fig.4 shows the actual missions for constant burn-out time and different θ_0

It is clear that the attitude errors for different missions have settled to within 2 degrees in a settling time of approximately one-third of the burn-out time.

3-THRUST UNCERTAINTY FORMULATION

The total impulse of the solid propellant rocket motor depends on the chemical compound and the burning rate. The thrust-time profile depends on the form function and the environmental conditions of burning. The burn-out time depends on the form function and the burning rate, so it is also uncertain. Accordingly, the thrust profile may suffer from uncertainties due to production tolerances and off-nominal environmental conditions. These uncertainties can be formulated as randomness in the profile shape parameters.

For the present study the simplified thrust-time curve shown in Fig.5 is considered, where:

$-F_1$ (initial thrust value), M_1 (slope of the segment F_1F_2), S_1 (area under the segment F_1F_2), and S_2 (the remaining area) are considered as Gaussian distributed random variables. Random function generators are used to generate F_{1i} , M_{1i} , S_{1i} , and S_{2i} where i is the trial number.

A population of 100 samples is simulated and the limiting curves are shown in Fig.5. The corresponding distribution of t_b is shown in Fig-6. where the random variations in t_b are within 2 seconds. The generated thrust-time profiles (100 trials) are sorted w.r.t. t_b in an ascending order and for each case the impact range is calculated through a 3-dimensional simulation procedure. As shown in Fig.7, it was found that r_{1imp} decreases with increasing t_b and that the variation in r_{1imp} is within 0.2 %.

The determination of t_{imp} can be carried out through:

- 1-nominal trajectory off-line simulation
- 2-statistical means
- 3-software sensor

For the present case study, the components of the gravitational acceleration G_{e1} , G_{e2} are nearly constant for a specific mission, i.e their variation with respect to time is negligible, but they may differ from nominal .

4-GUIDANCE CORRECTION ALGORITHM

4.1-Simplified Free Space Fire Plane Motion Equations

Under the assumption that:

-launch point is at (0,0)

thus : $r_1(t) = x_e(t)$

$r_2(t) = y_e(t) - R_e$

-target point in the north direction

-earth gravity components $G_{e1} = 0$; $G_{e2} = -g_0$.

the free space fire plane motion equations are:

$$\dot{r}_1 = v_{e1} \quad \dot{r}_2 = v_{e2} \quad \dot{v}_{e1} = 0 \quad \dot{v}_{e2} = -g_0$$

$$\dot{w}_{z1} = 0$$

$$\dot{I}_1 = 0$$

$$\dot{I}_2 = 0$$

$$\dot{J}_1 = 0$$

$$\dot{J}_2 = 0$$

with initial conditions:

$$r_1(0) = r_{1b} \quad r_2(0) = r_{2b} \quad v_{e1}(0) = v_{e1b} \quad v_{e2}(0) = v_{e2b}$$

$$w_{z1}(0) = 0$$

$$I_1(0) = I_{1b} \quad I_2(0) = I_{2b} \quad J_1(0) = J_{1b} \quad J_2(0) = J_{2b}$$

Hence; the states affecting the free space ballistic missile motion are $r_1(t)$, $r_2(t)$, $v_{e1}(t)$, $v_{e2}(t)$.

14-16 May 1991, CAIRO

4.2- Solution of the equations describing the free space missile motion in the fire plane ;

The solution of the above system of equations represents a look ahead predictor for t_{imps} , r_{imps} at t_b as follows:

$$\begin{aligned} r_1(t) &= r_{1b} + (t-t_b)V_{e1b} \\ r_2(t) &= r_{2b} + (t-t_b)V_{e2b} - 1/2 g_o(t-t_b)^2 \\ V_{e1}(t) &= V_{e1b} \\ V_{e2}(t) &= V_{e2b} - g_o(t-t_b) \end{aligned}$$

at $t = t_{imp}$:

$$\begin{aligned} r_{1imps} &= r_{1b} + (t_{imps}-t_b)V_{e1b} \\ r_{2imps} &= r_{1b} + (t_{imps}-t_b)V_{e2b} - 1/2 g_o(t_{imp}-t_b)^2 \\ t_{imps} &= t_1 + 2r_2(t_1)/g_o \end{aligned}$$

$$\begin{aligned} \text{where: } t_1 &= t_b + v_{e2b}/g_o \\ r_2(t_1) &= r_{2b} + (t_1-t_b)v_{e2b} - \frac{1}{2}g_o(t_1-t_b)^2 \end{aligned}$$

4.3-The Nature of r_{imps} , t_{imps}

For the specified mission ($\theta_o = 60^\circ$), and through one hundred shootings (for t_b sorted in an ascending order), the performance of the proposed software algorithm is compared with that yielded by the complete time-varying developed mathematical model (actual performance); Figures 7 and 8. It was found that r_{imps} and t_{imps} are nearly constant with respect to t_b similar to the actual r_{imp} and t_{imp} , nevertheless there is some error (nearly constant w.r.t. t_b). This error can be minimized by:

- more accurate representation of the gravity model.
- more accurate calculation of t_{imp} taking into consideration the spherical shape of the earth (G_{e1} and G_{e2})
- making use of perturbation technique

4.4-Burn-out impact point transition perturbations :

$$\delta r_{1imp} = \delta r_{1b} + (t_{imp}-t_b)\delta V_{e1b}$$

$$\delta r_{2imp} = \delta r_{2b} + (t_{imp}-t_b)\delta V_{e2b}$$

4.5 Guidance Correction Demand Formulation

For annulling the error at impact ($\delta r_{1imp}=0$; $\delta r_{2imp}=0$) then :

$$0 = \delta r_{1b} + (t_{imp}-t_b)\delta V_{e1c}$$

$$0 = \delta r_{2b} + (t_{imp}-t_b)\delta V_{e2c}$$

where:

δV_{e1c} , δV_{e2c} are the command perturbations;

$$\delta V_{e1c} = \frac{-\delta r_{1b}}{t_{imp}-t_b} \quad ; \quad \delta V_{e2c} = \frac{-\delta r_{2b}}{t_{imp}-t_b}$$

According to Fig.2 the mission is described by Γ_r , and the guidance correction demand will be formulated as follows:

$$\Gamma = \tan^{-1} (v_{e2} / v_{e1}) \quad ; \quad \dot{\Gamma} = \frac{v_{e1} \dot{v}_{e2} - v_{e2} \dot{v}_{e1}}{v_{e1}^2 + v_{e2}^2}$$

$$\delta \dot{\Gamma} = \left[\frac{\dot{v}_{e2}}{v_{e1}^2 + v_{e2}^2} - \frac{2v_{e1}(v_{e1}\dot{v}_{e2} - v_{e2}\dot{v}_{e1})}{(v_{e1}^2 + v_{e2}^2)^2} \right] \delta v_{e1c} +$$

$$\left[\frac{-\dot{v}_{e1}}{v_{e1}^2 + v_{e2}^2} - \frac{2v_{e2}(v_{e1}\dot{v}_{e2} - v_{e2}\dot{v}_{e1})}{2(v_{e1}^2 + v_{e2}^2)} \right] \delta v_{e2c} -$$

$$\left[\frac{v_{e2}}{v_{e1}^2 + v_{e2}^2} \right] \delta \dot{v}_{e1} + \left[\frac{v_{e1}}{v_{e1}^2 + v_{e2}^2} \right] \delta \dot{v}_{e2}$$

$\delta \dot{\Gamma}_r$ is calculated for $t \geq t_{bso}$

5-RESULTS

For evaluating the proposed guidance correction algorithm the impact accuracy is used as a criterion.

Fig.9. illustrates the impact error δr_{limp} , versus burn-out time, for uncompensated and compensated cases respectively.

Fig.10. shows the impact error distribution for both cases. The corresponding statistical parameters can be summarized as follows

Impact Error	Uncompensated	Compensated
Mean (M)	1.044	0.001
Dispersion(σ)	0.460	0.160
CEP %	0.306	0.037

6-CONCLUSION

Due to production tolerances and off-nominal environmental conditions, solid propellant thrust time profile has a random character in both magnitude and burn out time. This character leads to uncertainties in the motion parameters near burn out, and consequently the impact point is highly erroneous.

The proposed guidance correction algorithm compensates for these uncertainties through transition relations relating the perturbations near burn out to the impact error. The CEP is improved about 10 times and with some sophistications more improvements are attainable.

REFERENCES

- [1] J.W. CornLisse, H.F.R.Schoyer and K.F.Wakker, "Rocket propulsion and Space Flight Dynamics." Pitman publishing Limited, 1979.
- [2] George R.Pitman, JR., "Inertial Guidance." John Willey & Sons, New York 1962.
- [3] Arthur L.Greensite, " Analysis and Design of Space Vehicle Flight Control Systems " Spartan Books, New York, 1970
- [4] Hideo Ikaw, " A unified Three Dimensional Trajectory Simulation Methodology. J.Guidance & Control, vol.9, No.6, 1986.
- [5] K.R.Britting, "Navigation Analysis", Willy Interscience, 1971.
- [6] Elleithy, Tantawy, Ghoniemy, " Development of a six degrees of freedom model for surface to surface strapdown ballistic missiles." , Third ASAT Conference, MTC, Cairo, Egypt, 1989
- [7] W.Templman, " Linear Guidance Laws For Space Missions". The Charles Starck Droper Laboratory, Inc. 552 Technology Square, Cambridge, Massachusetts 02139., American Institute of Aeronautics and Astronautics Inc. 85- 1915, 1985.
- [8] Jhon W.Hardtler, Michael J.Plehhler Jerre E.Bradt, " Guidance Requirements For Future Launch Vehicle" American Institute of Aeronautics and Astronautics, Inc., 87-2462, 1987.
- [9] Salem A.K.Al-Assadi and Lamya A.M.Al chalabi, "Optimal Gain For Proportional Integral Derivative Feedback "IEEE Control Systems Magazine P 17-19, December 1987.

NOMENCLATURE

$Ox_e y_e z_e$	=Geocentric earth fixed (centered) reference frame
$Lx_1 y_1 z_1$	=Body fixed frame
I_m	=Unit vector in direction of x_1 with components I_1, I_2, I_3^*
J_m	=Unit vector in direction of y_1 with components J_1, J_2, J_3^*
K_m	=Unit vector in direction of z_1 with components K_1, K_2, K_3^*
θ_0	=Initial launch elevation angle
ψ_0	=Initial Launch azimuth angle
R_m	=Missile range vector with components x_e, y_e, z_e^*
R_e	=Earth equatorial radius (6378165 meters)
V_e	=Missile velocity vector with components v_{e1}, v_{e2}, v_{e3}^*
A_e	=Missile specific force vector of components A_{e1}, A_{e2}, A_{e3}^*
ω_e	=Earth rotation angular speed $=7.2921 \cdot 10^{-5}$ rad/sec.
ω_m	=Missile angular rate vector
ω_{me}	=Missile angular rate vector *
V_a	=Missile velocity vector
A	=Missile specific force vector with components A_1, A_2, A_3
G_e	=Gravitational field vector with components G_{e1}, G_{e2}, G_{e3}^*
g_0	=Gravitational acceleration (9.8 m/sec^2)

- Γ
- H_a =Missile angular momentum vector = $J \cdot \omega_m$
- J =Missile moment of inertia w.r.t. its axes
- F_A =Aerodynamic force vector
- F_T =Thrust force vector
- Γ_A =Aerodynamic moment vector
- Γ_T =Thrust moment vector
- mass =Missile mass
- Γ =Flight path tangent angle
- Γ_0 =Mission flight path angle
- Γ_r =Real flight path tangent angle
- F_0 =Magnitude of total thrust of rocket motor [$kg \cdot m/sec^2$]
- t_b =Burn out time
- t_{imp} =Impact time at target
- t_{imps} =Impact time predicted by the proposed algorithm
- r_{1b} =Burn out downrange
- r_{2b} =Burn out height
- v_{e1b} =Burn out down velocity
- v_{e2b} =Burn out height velocity
- r_{1imp} =Down impact range
- r_{1imps} =Down impact range predicted by the proposed algorithm
- r_{2imp} =Height impact range
- r_{2imps} =Height impact range predicted by the proposed algorithm
- δ_z =Nozzle deflection
- U_d =Control demand
- t_{bso} =Starting time for correction
- CEP =Circular propable error
- $*$ =in earth coordinate system

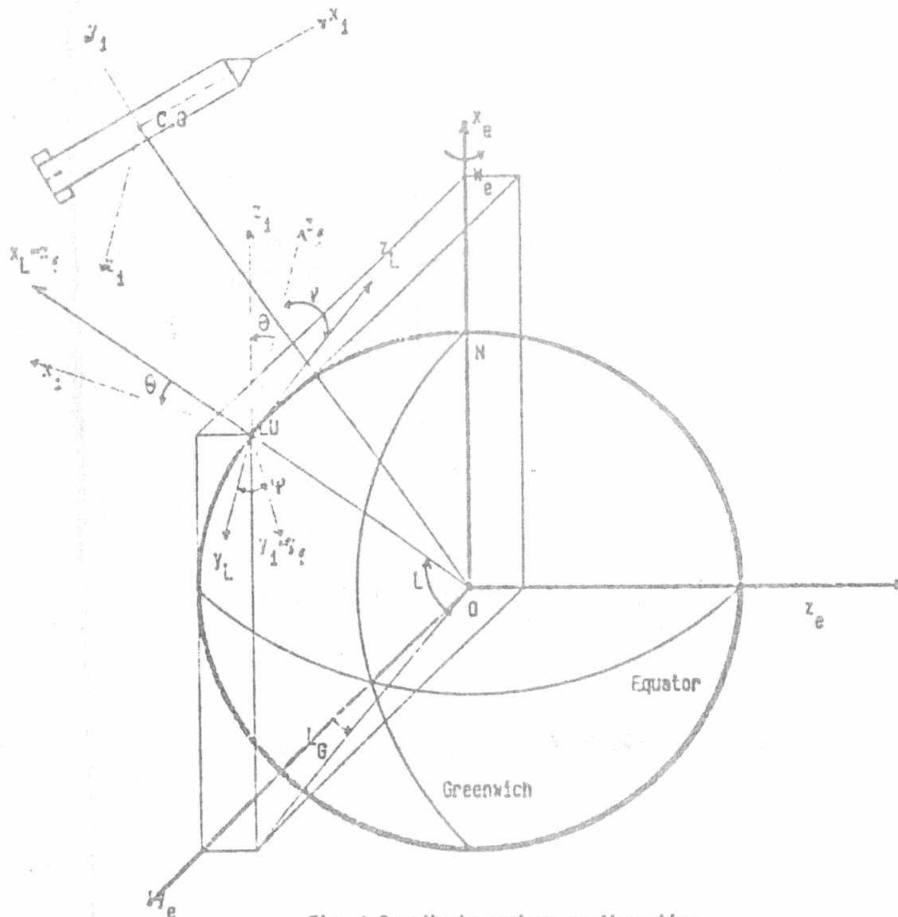


Fig. 1 Coordinate systems configuration

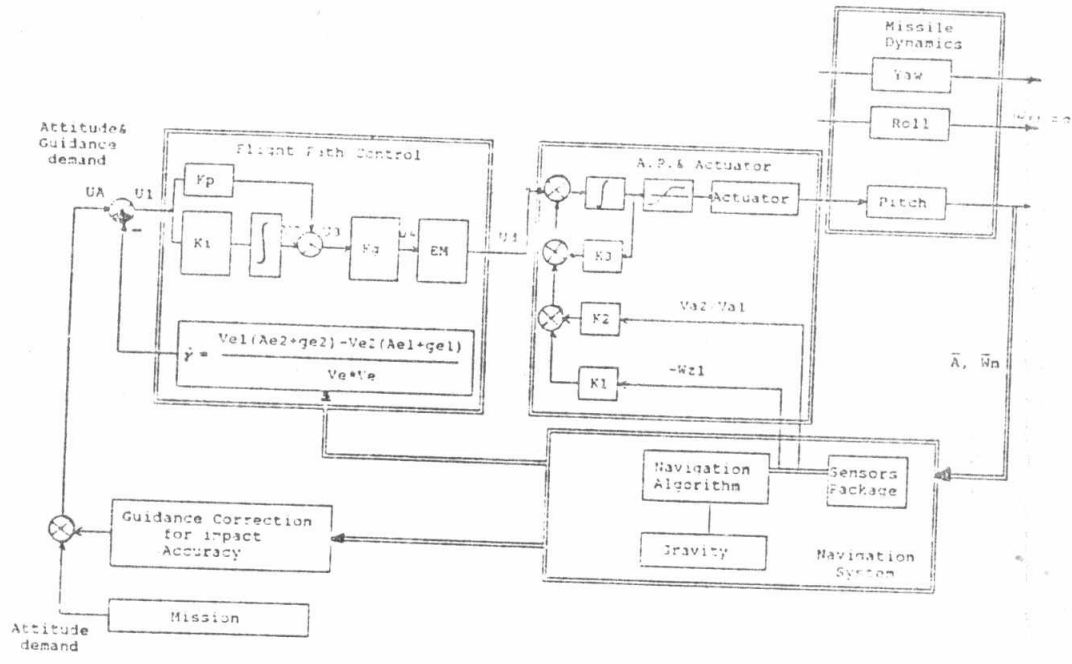


Fig.2. Ballistic Missile Control Scheme in the Fire Plane

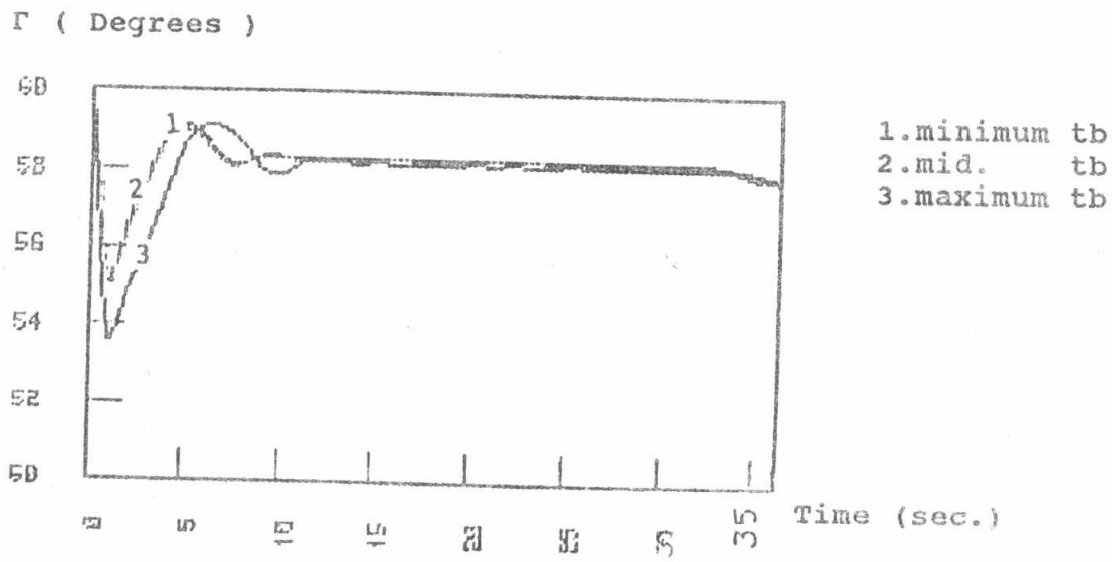


Fig.3. Flight path response for different tb

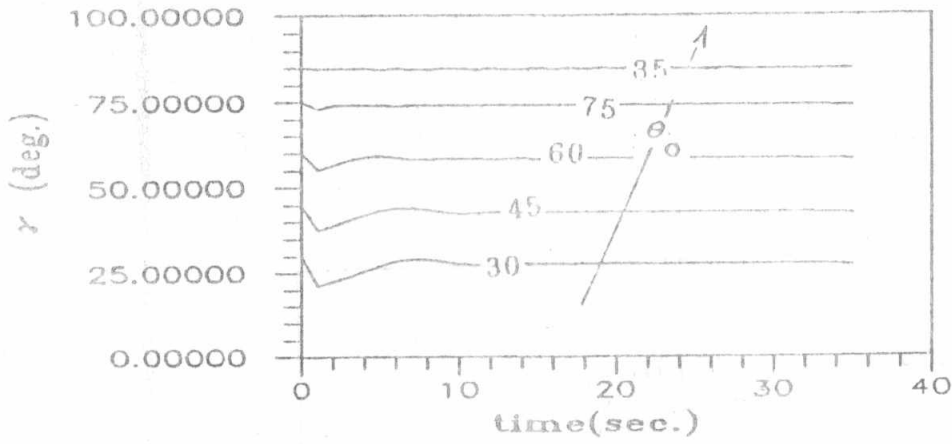


Fig.4. Flight path response for different missions

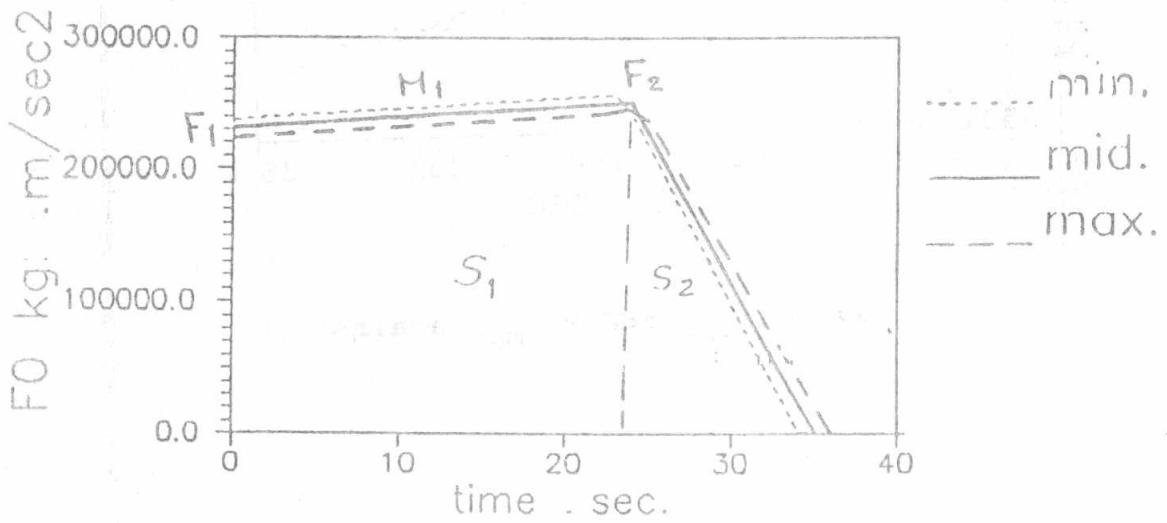


Fig.5. Simulated thrust

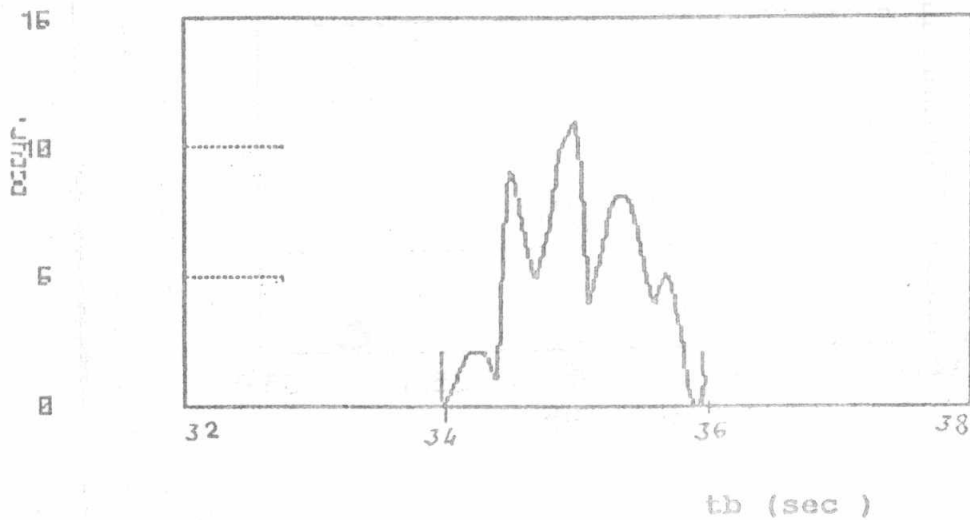


Fig.6. tb Distribution

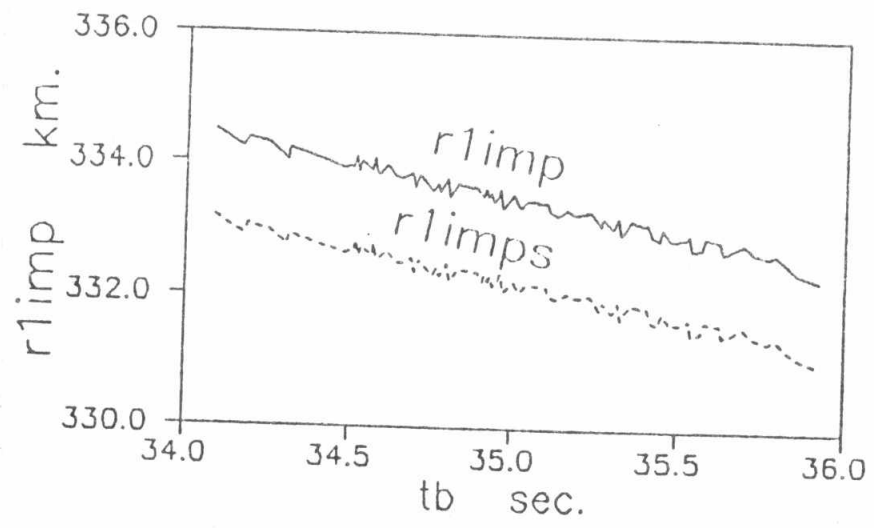


Fig.7. r_{1imp} and r_{1imps} against tb

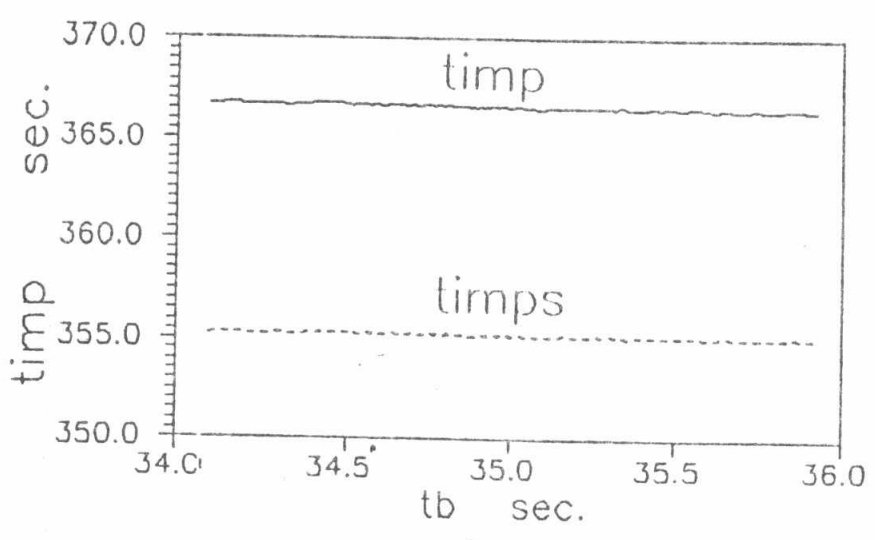


Fig.8. t_{imp} and t_{imps} against tb

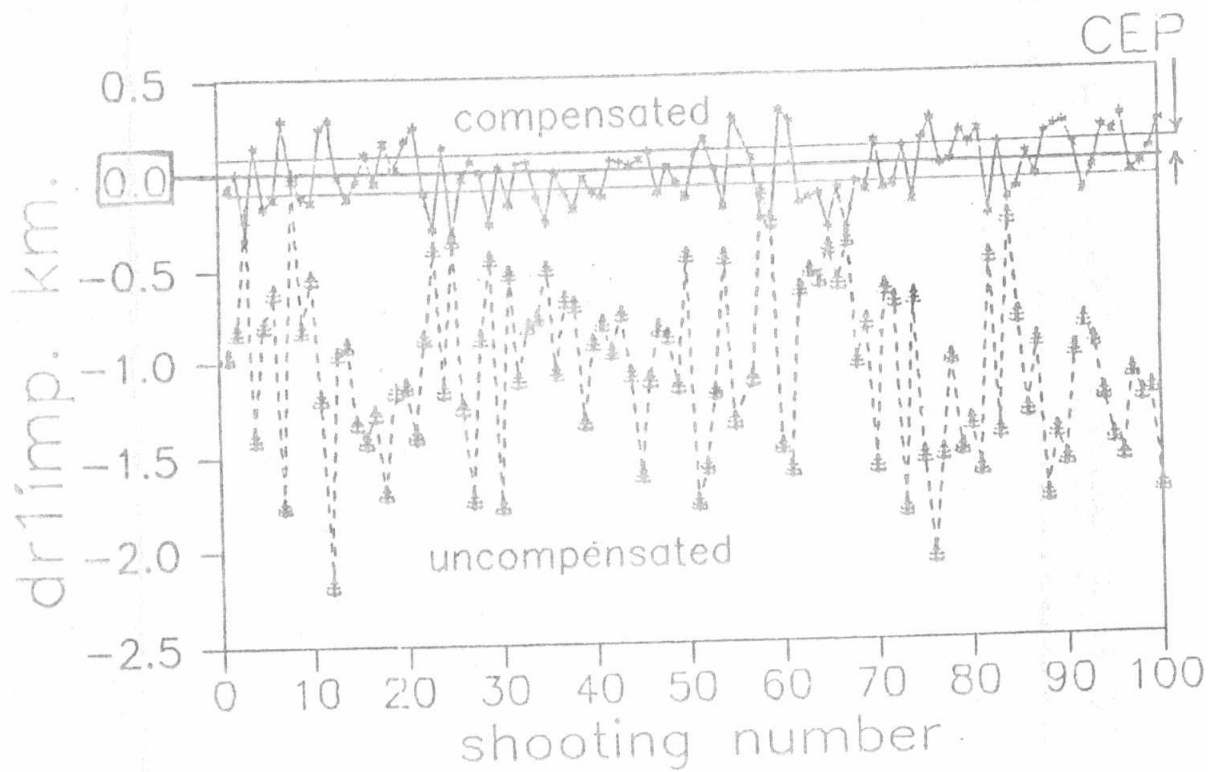


Fig.9. Impact error evaluation

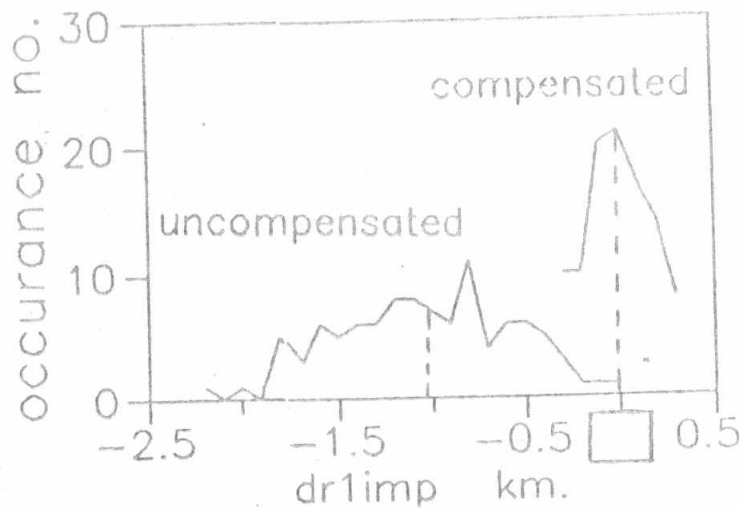


Fig.10. Impact error distribution